

Charge Regulating Macro-ions in Salt Solutions: Screening Properties and Electrostatic Interactions

Yael Avni,¹ David Andelman,^{1,*} Tomer Markovich,^{1,2} and Rudolf Podgornik^{3,†}

¹*Raymond and Beverly Sackler School of Physics and Astronomy,
Tel Aviv University, Ramat Aviv 69978, Tel Aviv, Israel*

²*DAMTP, Centre for Mathematical Sciences, University of Cambridge, Cambridge CB3 0WA, United Kingdom*

³*School of Physical Sciences and Kavli Institute for Theoretical Sciences,
University of Chinese Academy of Sciences, Beijing 100049, China and
CAS Key Laboratory of Soft Matter Physics, Institute of Physics,
Chinese Academy of Sciences, Beijing 100190, China*

(Dated: April 9, 2018)

We revisit the charge-regulation mechanism of macro-ions and apply it to mobile macro-ions in a bathing salt solution. In particular, we examine the effects of correlation between various adsorption/desorption sites and analyze the collective behavior in terms of the solution effective screening properties. We show that such a behavior can be quantified in terms of the charge *asymmetry* of the macro-ions, defined by their preference for a non-zero effective charge, and their *donor/acceptor* propensity for exchanging salt ions with the bathing solution. Asymmetric macro-ions tend to increase the screening, while symmetric macro-ions can in some cases decrease it. Macro-ions that are classified as donors display a rather regular behavior, while those that behave as acceptors exhibit an anomalous non-monotonic Debye length, where a sharp change in the screening can occur as a function of a small change in the salt concentration. The screening properties, in their turn, engender important modifications to the disjoining pressure between two charged surfaces. Our findings are in particular relevant for solutions of proteins, whose exposed amino acids can undergo charge dissociation/association processes to/from the bathing solution, and can be considered as solution of charged regulated macro-ions, as considered here.

I. INTRODUCTION

Long-range interactions between biological macromolecules are similar in many respects to those that characterize inorganic colloids. Following the Deryaguin-Landau-Verwey-Overbeek (DLVO) paradigm [1], the interactions can be decomposed into the van der Waals and the electrostatic components [2, 3]. However, more complex examples of colloids with *ionizable groups*, or proteins with ionizable amino-acid residues [4–6] differ substantially from colloids that carry a fixed charge [7]. Dissociation of such chargeable moieties engenders an exchange of ions (usually but not necessarily, a proton, H^+) with the bathing solution [8, 9]. Consequently, it changes the nature of protein-protein interactions [10, 11], and modifies the protein-specific spatial charge distribution [5, 12, 13].

The exchange of ions between proteins (via their dissociable groups) and the surrounding solution has been addressed already in the 1920's by Linderstrøm-Lang of the Carlsberg Laboratory [14]. Later on, it was referred to as the *charge regulation* (CR) mechanism, and its formalism was set fourth by Ninham and Parsegian [15]. In their seminal 1971 work, CR was formulated within the

Poisson-Boltzmann (PB) theory of electrostatic interactions in an aqueous environment [1], which included an additional self-consistent boundary condition at the CR bounding surfaces. In recent decades, the CR formulation was implemented for surface binding sites via the law of mass action [16–19], and separately, by modifying the surface free-energy [20–30]. The latter approach leads to the same surface dissociation equilibrium as does the law of mass action, but with the advantage that it can be easily generalized to include other non-electrostatic surface interactions.

The charge association/dissociation process (CR mechanism) couples the local electrostatic field with the local charge, and results in a partition of dissociated and associated states, which is obtained self-consistently [30]. This local coupling implies a complex dependence of the net charge of the macro-ion, protein or proteinaceous aggregate on the solution conditions, the local dielectric profiles and the overall system geometry [31]. Furthermore, in some cases, higher-order electrostatic multipoles may need to be considered in relation to the CR process, in addition to its monopolar ones [13].

The PB theory with CR charges was studied in the past for planar geometries of one or two charged-regulating surfaces, in contact with a bathing electrolyte solution, or by modeling a charged colloid in solution, in the proximity of another charged surface [30, 32–34]. Other, more complicated and realistic geometries of protein-protein interactions in different aqueous solution environments have also been studied by various simulation techniques [35, 36]. A viable simplification of the above

* andelman@post.tau.ac.il

† Also affiliated with the Department of Physics, Faculty of Mathematics and Physics, University of Ljubljana, and with the Department of Theoretical Physics, J. Stefan Institute, 1000 Ljubljana, Slovenia

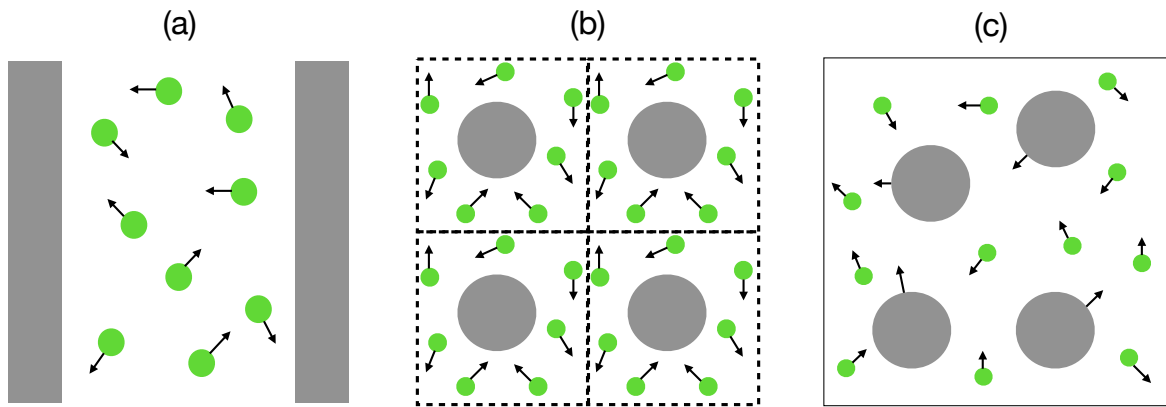


FIG. 1. (color online) A schematic illustration of different approaches to model charge regulating macro-ions (gray) in an ionic solution (green). (a) The macro-ions are approximated by flat bounding surfaces, with salt ions moving between them. (b) Each macro-ion is fixed in a cell with mobile salt ions within the cell. The interaction between the neighboring macro-ions is mimicked by the boundary conditions of the cell. (c) Both the salt ions and macro-ions are free to move in the entire system. While (a) and (b) were modeled and analyzed extensively in the past, our theory strives to describe the latter case (c), which is the only one that accounts for the collective behavior of the macro-ions.

problem is described by a variant of the *cell model* [37–40], where the macro-ion is enclosed within an external cell, whose boundary conditions mimic the presence of neighboring macro-ions,

We note that the cell model, as well as the other CR works mentioned above, neglects the translational entropy of the macro-ions, and can be justified only when the salt concentration is high enough, such that collective many-body effects become irrelevant. In the opposite limit, when the translational degrees of freedom of macro-ions and salt ions are strongly coupled, one needs to employ a more refined and collective description. To this effect, a model based on the PB framework has been recently developed by us [41] to account for these collective CR effects for *mobile* macro-ions in dilute salt solutions. The model deals with charge regulating macro-ions and simple salt ions on an equal footing (see Fig. 1). As an example, it was implemented so far only for a single, specific CR model of the macro-ions.

Motivated by the recent studies of charge regulation of nonpolar colloids [42], we now extend our approach [41] by studying in detail different generalized CR models of mobile macro-ions in electrolyte solutions. The main focus is on *zwitterionic* macro-ions, *i.e.*, dissociable macro-ions that contain both positive and negative charge states. For example, proteins with protonation/deprotonation of chargeable solvent exposed amino acids. In such cases, the more subtle coupling between the charge regulating macro-ions and the fully dissociated salt ions leads to completely unexpected and important modifications of the usual behavior of such charged systems.

Hereafter, we present a few intriguing examples where the effective screening length exhibits a *non-monotonic* and sharp dependence on both the salt and the charge regulating macro-ion bulk concentrations. The mechanism responsible for this behavior is unraveled in terms

of the charge asymmetry of the macro-ions and their *donor/acceptor* propensity. Furthermore, the disjoining pressure between two charged surfaces is shown to exhibit a non-monotonic dependence on the macro-ion bulk concentration at a fixed separation between the surfaces. These unexpected features of dissociating macro-ions shed new light on the understanding of electrostatic interactions in complex colloid systems.

The outline of our paper is as follows. In Sec. II, we present the general approach of treating a solution containing mobile CR macro-ions, and present its the free energy. We then introduce in Sec. III two generic types of CR mechanisms for zwitterionic macro-ions, and obtain the corresponding mean-field description of their electrostatic interactions. We further calculate the modified screening length and disjoining pressure as applied to two charged planar surfaces immersed in solutions containing mobile CR macro-ions. In Sec. IV, we conclude with several more general observations of our results and remarks about connection to existing experiments and suggest future ones.

II. THE CHARGE-REGULATING MODEL

Our model system is composed of monovalent salt ions in an aqueous solvent with dielectric permittivity ϵ at temperature T . Macro-ions are added to the solution in the form of colloidal particles with active charge groups, enabling the desorption/adsorption of monovalent ions to/from the solution. For simplicity, the dissociating ions are assumed to be of the same type as the salt ions, so there are only two types of small ions in solution: monovalent cations and anions. This assumption simplifies the calculation but can be easily relaxed by rather minor modifications to the model.

Before macro-ions are added to the aqueous solution, they are assumed to be neutral. As they are put in contact with the bathing solution, they become charged because of the dissociation process. It is convenient to define the bulk concentration of the monovalent salt (prior to the addition of macro-ions) as n_0 , and the bulk concentration of the added macro-ions as p_b because these are the two experimentally controllable parameters. Note that after the macro-ions are added and equilibrate with the ionic solutes, the bulk cation and anion concentrations differ from n_0 . We define them as n_b^+ and n_b^- , and they depend on n_0 as well as on p_b . We will see that this dependence hinges on the details of the CR model and is different for the two specific CR models considered below.

For clarity sake, we assume that the solvent molecules and salt ions have the same volume, a^3 , whereas the macro-ion specific volume is written as γa^3 , where $\gamma > 1$ is a numerical pre-factor describing the ratio between the two molecular volumes. As the effective radius of a protein is typically 1 – 5 nm for molecular weights in the range of 5 – 500 kDa [43], while the simple salt ions have a typical size of ~ 0.3 nm, the corresponding γ has values up to $\sim 10^3$. Much higher values of γ would have to be considered for CR nano-particles, entailing a consistent inclusion of packing effects at higher concentrations, a direction that we will not pursue further in this work.

In the dilute limit of both solutes (salt and macro-ions), the entropy can be approximated by the ideal entropy of mixing

$$S/k_B = - \sum_{i=\pm} n_i [\ln(n_i a^3) - 1] - p [\ln(p \gamma a^3) - 1], \quad (1)$$

while the total mean-field free energy, $F = U - TS$ has the form [1, 41, 44]:

$$F = \int_V d^3r \left[- \frac{\varepsilon}{8\pi} (\nabla\psi)^2 + e(n_+ - n_-)\psi - TS + pg(\psi) - (\mu_+ n_+ + \mu_- n_- + \mu_p p) \right], \quad (2)$$

where $n_{\pm}(\mathbf{r})$ and $p(\mathbf{r})$ are the number densities at position \mathbf{r} of the small \pm ions and macro-ions, respectively, k_B is the Boltzmann constant, $\psi(\mathbf{r})$ is the local electrostatic potential, μ_{\pm} are the chemical potentials of the monovalent ions and μ_p for the macro-ions. The macro-ion term in the above expression is given by the single macro-ion free energy, $g(\psi)$, that characterizes the specific CR process. The functional dependence of $g(\psi)$ on other system parameters differs for different models that we consider. In fact, this is the only non-standard term of Eq. (2), first introduced in Ref. [41] and shown to have significant consequences.

As the CR processes take place on the surface of the macro-ion located at position \mathbf{r} , the corresponding $g(\mathbf{r})$ can be written as

$$g(\mathbf{r}) = \oint_S d^2\mathbf{r}' g_s(\mathbf{r} + \mathbf{r}'), \quad (3)$$

where the form of the surface free-energy $g_s(\mathbf{r})$ is identical to that used in the CR models formulated for dissociable surfaces, and can assume various forms including Langmuir-Davies and Langmuir-Frumkin-Davies isotherms [1, 29, 30, 45]. We exploit the fact that as long as the inter-particle typical distances are larger than the macro-ions size ($p\gamma a^3 \ll 1$, $n_{\pm}\gamma a^3 \ll 1$), $g_s(\mathbf{r})$ can be approximated by its value at the center of the macro-ion and $g(\mathbf{r})$ can be treated as a purely local function at position \mathbf{r} . When the inter-particle distances are comparable to the macro-ion size, one would need to retain not only the finite size of the macro-ions but also the non-uniform distribution of sites along their surface.

The thermodynamical equilibrium is obtained by using the variational principle for F with respect to all the thermally annealed variables: the three densities n_{\pm}, p , the potential ψ , and the fraction of associated ions, to be introduced in the next section. However, the variation with respect to the three densities and electrostatic potential can be taken without any prior knowledge of g .

From $\delta F/\delta n_{\pm} = 0$, it follows that the ion densities n_{\pm} satisfy the Boltzmann distribution,

$$n_{\pm}(\psi) = n_b^{\pm} e^{\mp\beta e\psi}, \quad (4)$$

with $n_b^{\pm} = \exp(\beta\mu_{\pm})/a^3$ defined as the cation/anion bulk concentration, taken at zero reference potential, $\psi = 0$.

Next, the variation principle of F , $\delta F/\delta p = 0$, gives the Boltzmann distribution for the macro-ion concentration,

$$p(\psi) = p_b e^{\beta[g(\psi) - g_0]}, \quad (5)$$

where $g_0 = g(\psi = 0)$ acts as a reference bulk state with $\psi = 0$, and the bulk density of the macro-ion p_b satisfies $p_b = \exp(\beta\mu_p + \beta g_0)/\gamma a^3$.

The variation of F with respect to ψ finally yields a generalized Poisson-Boltzmann equation,

$$-\frac{\varepsilon}{4\pi} \nabla^2 \psi = \rho(\psi) = e(n_+(\psi) - n_-(\psi)) + Q(\psi)p(\psi) \quad (6)$$

where the effective charge of each macro-ion is defined as

$$Q = \frac{\partial g(\psi)}{\partial \psi}. \quad (7)$$

Note that if the macro-ions were simple ions of valency $\pm z$, the effective charge would be $Q = \pm ze$. Consequently, g would have the usual form $\pm ez\psi$, and Eqs. (5)-(7) would reduce to the standard form of the Poisson-Boltzmann equation.

III. RESULTS AND DISCUSSION

We present our results for two different CR models, each with its own assumptions leading to a distinct macro-ion free energy, $g(\psi)$. The variation of the free energy as in Eqs. (4)-(7) together with the variation with respect to the CR degrees of freedom on the macro-ions, leads to a complete set of equations of state for the two

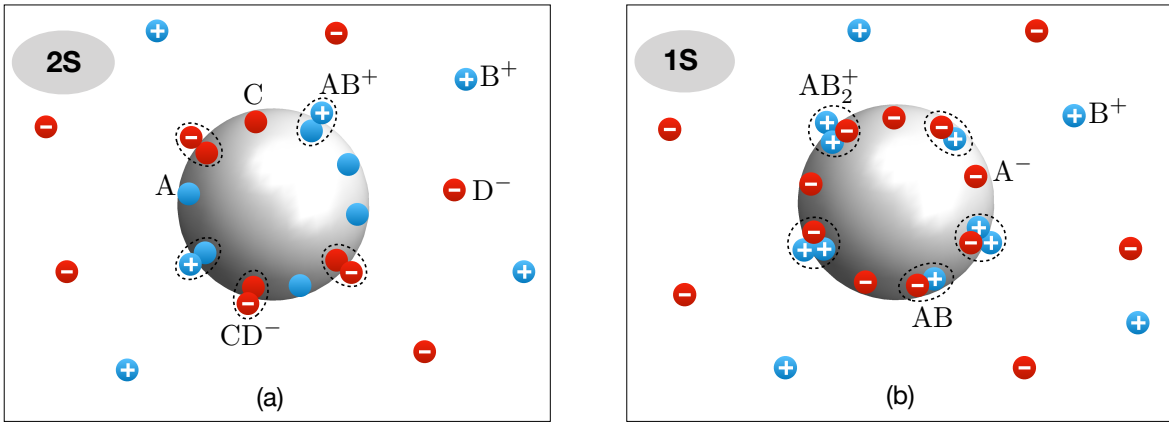
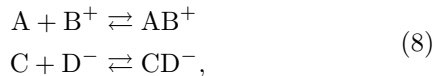


FIG. 2. (color online) The two charge regulation models, 2S and 1S, described by Eqs. (8) and (21), respectively. (a) In the 2S model, each macro-ion has two types of surface dissociable sites, A and C. The A site can adsorb/desorb a cation (B^+), while the C site can adsorb/desorb an anion (D^-). During the adsorption process, the neutral A site acquires a positive charge, becoming AB^+ , while the neutral C site becomes negatively charged as CD^- . (b) In the 1S model, only cations can be absorbed from solution. The macro-ion carries only one type of active surface sites, and each such site has three charging states. (i) It can stay neutral in its native AB state; (ii) it can release a cation (B^+) and become negative (A^-); or, (iii) it can adsorb a cation (B^+) and become positive ($A^-B_2^+$).

CR models. By solving them, we can get insightful predictions about the screening length and the disjoining pressure between two charged surfaces.

A. The two-site (2S) model

We consider as our first CR model the case where the zwitterionic macro-ions contain two types of active sites: one that can adsorb/desorb a cation from/to the solution, and the other site that can adsorb/desorb an anion (see Fig. 2(a)). This adsorption model, involving two distinct types of active sites, is denoted hereafter as the *2S model*. It is described by the chemical reaction equations:



where A and C represent two active macro-ion sites. The charges, B^+ and D^- are, respectively, monovalent cation and anion, which can be released to the solution or bind onto the macro-ion from the solution (see Fig. 2(a)). A possible realization of such a process involving a proton H^+ and a hydroxyl group OH^- is described in Ref. [46].

We assume that each macro-ion contains N_+ potentially dissociable A sites and N_- dissociable C sites. Note that only a fraction of the overall N_{\pm} sites will become charged at any given solution conditions. This fraction is introduced below as ϕ_{\pm} . Furthermore, the A and C active sites are uncorrelated in any direct manner.

In the 2S model, the free energy of a single macro-ion,

$g(\psi)$, is assumed to be given by

$$\begin{aligned} g^{2S}(\psi, \phi_+, \phi_-) &= \sum_{i=\pm} N_i \phi_i (e_i \psi - \mu_i - \alpha_i) \\ &+ k_B T \sum_{i=\pm} N_i \left(\phi_i \ln \phi_i + (1 - \phi_i) \ln(1 - \phi_i) \right), \end{aligned} \quad (9)$$

where ϕ_+ (ϕ_-) is the number fraction of the total N_+ (N_-) sites that adsorb a cation (anion) from solution, and α_{\pm} is the free-energy change in adsorbing a cation/anion, respectively. If $\alpha_{\pm} > 0$, it means that there is a free-energy gain of association while a negative α_{\pm} opposes such binding.¹

We can now take the variation of F with respect to the occupied ionic fractions ϕ_{\pm} , $\delta F / \delta \phi_{\pm} = 0$. This gives the Langmuir-Davies isotherm [27, 45]

$$\phi_{\pm} = \frac{Z_{\pm}^{2S}(\psi) - 1}{Z_{\pm}^{2S}(\psi)}, \quad (10)$$

where

$$Z_{\pm}^{2S} = 1 + n_b^{\pm} K_{\pm} e^{\mp \beta e \psi}, \quad (11)$$

is the 2S partition function of a single macro-ion, and throughout the remaining of this subsection we shall omit the superscript 2S. In the above equation, we expressed Z_{\pm} in terms of the chemical equilibrium constants, K_{\pm} [1, 46],

$$K_{\pm} = a^3 e^{\beta \alpha_{\pm}}. \quad (12)$$

¹ Note that the model analyzed in Ref. [41] is a special case of the 2S model. It can be obtained in the following special limit: $N_+ = 2N_-$ and $\alpha_- \rightarrow \infty$, so that for negative charges $\phi_- = 1$.

Note that each of the K_{\pm} varies between zero and infinity corresponding to α_{\pm} varying between $-\infty$ and ∞ . The meaning of the limit $K_{\pm} \rightarrow \infty$ (or $\alpha_{\pm} \rightarrow \infty$) is that all active sites are fully associated and charged ($\phi_{\pm} \rightarrow 1$). Since in experiments only K_{\pm} is the measurable quantity, and not a or α_{\pm} separately, we will use hereafter K_{\pm} as the natural parameter in our numerical calculations and figures.

Substituting the expression for ϕ_{\pm} , Eq. (10), into Eq. (9), we obtain

$$g(\psi) = -k_B T \sum_{i=\pm} N_i \ln(Z_i). \quad (13)$$

Using Eqs. (5), (7) and (13), we write the macro-ion concentration $p(\psi)$ as

$$p(\psi) = p_b \left(\frac{Z_+(\psi)}{Z_+(0)} \right)^{N_+} \left(\frac{Z_-(\psi)}{Z_-(0)} \right)^{N_-}, \quad (14)$$

and its total charge, $Q(\psi)$

$$\begin{aligned} Q(\psi) &= Q_+ + Q_- = e(N_+ \phi_+ - N_- \phi_-) \\ &= e \left(N_+ \frac{Z_+(\psi) - 1}{Z_+(\psi)} - N_- \frac{Z_-(\psi) - 1}{Z_-(\psi)} \right). \end{aligned} \quad (15)$$

Combining Eqs. (14), (15) and (4), the local charge density of cations, anions and charged macro-ions can be written explicitly in terms of ψ ,

$$\rho(\psi) = e \left(n_b^+ e^{-\beta e \psi} - n_b^- e^{\beta e \psi} \right) + p(\psi) Q(\psi) \quad (16)$$

with $p(\psi)$ and $Q(\psi)$ given in Eqs. (14) and (15).

Finally, we express the bulk concentrations, n_b^{\pm} , of the two ionic species in terms of the two controllable parameters: the bulk salt concentration before the addition of the macro-ions, n_0 , and the bulk concentration of the macro-ions, p_b .

To that end, we need prior knowledge about the macro-ion's initial state. Although it is easiest to picture the macro-ions as having all of their sites completely neutral before dissolved in the solution, in realistic cases some sites can be charged, meaning that the macro-ions enter the solution with potentially dissociable sites. We define the number of initially occupied A and C sites on the macro-ion as P_0^+ and P_0^- , respectively. For simplicity, we assume that initially both the macro-ions as well as the bathing salt solution are overall electroneutral, *i.e.*, $P_0^+ = P_0^- \equiv P_0$. Therefore, the total number of monovalent ions per unit volume is $n_0 + p_b P_0$, and

$$n_b^{\pm} = n_0 + p_b [P_0 - N_{\pm} \phi_{\pm}(0)]. \quad (17)$$

The above form ensures that electro-neutrality is satisfied in the bulk, and is in agreement with the definition of n_b^{\pm} and n_0 presented in the beginning of Sec. II. Note that $\phi_{\pm}(0)$ depends on n_b^{\pm} via Eq. (10). Thus, Eq. (17) is quadratic in n_b^{\pm} , but it has only one physically admissible root.

B. Screening length for 2S model

After deriving the expressions for $n_{\pm}(\psi)$, $Q(\psi)$ and $p(\psi)$ in terms of the model parameters, we can analyze the effect of adding macro-ions and simple monovalent salt. A convenient way to proceed is by analyzing the effective screening length, λ_{eff} . It is obtained by expanding the generalized PB equation, Eq. (6), to the first order in the electrostatic potential, ψ ,

$$-\frac{\varepsilon}{4\pi} \nabla^2 \psi = \rho(\psi) \simeq \rho(0) + \rho'(0) \psi + \mathcal{O}(\psi^2), \quad (18)$$

and taking into account electroneutrality in the bulk, $\rho(0) = 0$. The equation that follows is equivalent to the standard Debye-Hückel equation, except that the role of the Debye screening length, λ_D , is played by the *effective screening length*, λ_{eff} ,

$$\lambda_{\text{eff}}^{-2} = -\frac{4\pi}{\varepsilon} \left. \frac{\partial \rho}{\partial \psi} \right|_{\psi=0}, \quad (19)$$

and in the absence of macro-ions, λ_{eff} reduces to the Debye screening length, $\lambda_D = 1/\sqrt{8\pi e^2 n_0 / (\varepsilon k_B T)}$.

To get the screening length in the 2S model, we substitute Eq. (16) into the above equation and take into account the electroneutrality condition, Eq. (17), wherefrom it follows that

$$\begin{aligned} \lambda_{\text{eff}} &= \lambda_D \left(1 + \frac{p_b}{n_0} P_0 + \frac{1}{2} \frac{p_b}{n_0} \frac{Q^2(0)}{e^2} \right. \\ &\quad \left. - \frac{1}{2} \frac{p_b}{n_0} [N_+ \phi_+^2(0) + N_- \phi_-^2(0)] \right)^{-1/2}, \end{aligned} \quad (20)$$

with ϕ_{\pm} and Q given by Eqs. (10) and (15), respectively. The positive second term is proportional to P_0 , defined in Sec. III.A above. This term demonstrates that the mobile ions that are initially released from the neutral macro-ion (proportional to P_0), increase the screening, as expected. The next terms depend on the number fractions ϕ_{\pm} and represent two different trends. The first of them, proportional to $Q^2(0)$, is positive and always increases the screening. The fourth and last term is negative and it decreases the screening. Nevertheless, it can be shown that the whole expression for the effective screening length is always positive, irrespective of parameter values.

When P_0 is much smaller than N_{\pm} , the second term in Eq. (20) can be safely neglected. In this case, “symmetrically” charged macro-ions, *i.e.*, $N_+ \phi_+ \approx N_- \phi_-$, have an overall vanishing charge and tend to decrease the screening. In the other case, “asymmetrically” charged ones, $N_- \phi_- \ll N_+ \phi_+$, for positively charged (or vice versa for negatively charged), increase the screening. This behavior is expected as symmetric macro-ions bind cations and anions, on average *in pairs*, thus diminishing the effective salt concentration and decreasing the screening. On the other hand, asymmetric macro-ions bind preferably either cations or anions but not both. In this process,

charged sites themselves start acting as screening agents, leading to an increase in screening.

Charge *asymmetry* of macro-ions appears as an important feature determining the effective screening and depends on the values of the K_{\pm} and N_{\pm} parameters. When $K_{+} \simeq K_{-}$ and $N_{+} \simeq N_{-}$, the macro-ions exhibit less charge asymmetry. We note that for charged polymers, the asymmetric case corresponds to net charged polyelectrolytes, while the symmetric one corresponds to polyampholytes, containing both positive and negative charged (zwitterionic) groups, which approximately balance each other [47].

In the limit of $P_0 \approx N_{\pm}$, the second term in Eq. (20) dominates the screening, with the charge asymmetry being less important. Note that when $P_0 > N_{\pm}\phi_{\pm}$, each macro-ion releases more ions than it adsorbs, while for $P_0 < N_{\pm}\phi_{\pm}$, the situation is reversed. Consequently, macro-ions can be classified as either *donors* or *acceptors*, where donors are more likely to increase the screening than acceptors. However, even a full acceptor, *i.e.*, a macro-ion with $P_0 = 0$, can increase the screening if it is asymmetric enough, as can be seen from the above analysis.

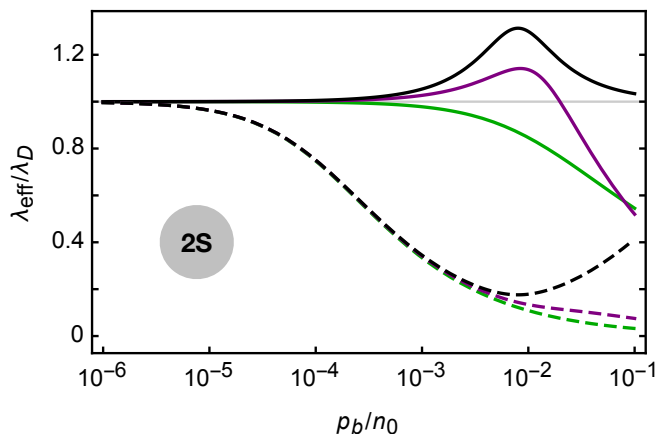


FIG. 3. (color online) The screening length in the 2S model, λ_{eff} , rescaled by the bare Debye screening length (no added macro-ions), λ_D , plotted as function of the macro-ion bulk concentration, p_b , rescaled by the bare salt concentration n_0 . The three top curves (solid lines) are plotted for the symmetric case of $n_0 K_{\pm} = 5$, while the dashed curves are plotted for the asymmetric case of $K_{+} \rightarrow 0$ and $n_0 K_{-} = 5$. We recall that the chemical equilibrium constant, K_{\pm} , is defined in Eq. (12). Three values of P_0 are shown with different colors: $P_0 = 0$ (black), $P_0 = 50$ (purple) and $P_0 = 150$ (green). For all cases, $N_{\pm} = 150$.

In Fig. 3 we plot λ_{eff} as a function of the macro-ion concentration, p_b (at fixed salt concentration, n_0), showing that the dependence of the screening length on p_b can be non-monotonic. However, as P_0 is increased, the non-monotonic behavior of λ_{eff} diminishes and eventually disappears. This can be understood by the following argument. Assume first that $P_0 = 0$. When the macro-ion concentration is small, they remove cations/anions from

the solution and decrease (or in some cases, increase) the screening, depending on their *charge asymmetry*, as explained above. This trend will continue until a saturation is reached at $p_b N_{\pm} \approx n_0$, where a substantial portion of the cations/anions are adsorbed onto the macro-ions (unless K_{\pm} have extremely small values). From that point on, every added macro-ion will get charged by removing cations or anions from the other macro-ions, and not only from the bulk, causing the number of cations and anions on each macro-ion to decrease. The asymmetric macro-ions then reverse their trend and become less screening. For symmetric macro-ions, the picture is more delicate: their overall charge remains zero, but the number of cations and anions is reduced. Surprisingly, this results in a decrease of the screening length (see Appendix A), and leads to the observed non-monotonic dependence. As we further increase P_0 , the macro-ions behave more like donors. The non-monotonicity eventually disappears because any added macro-ion contributes its own cations/anions to the solution, and does not only remove them from the solution.

This line of reasoning is further strengthened by the results plotted in Fig. 4. The macro-ion effective charge and the salt-ion charge density are shown as a function of the rescaled macro-ion concentration, p_b/n_0 . Figure 4(a) shows separately the positive charge $Q_{+} \equiv eN_{+}\phi_{+}$, the negative charge $Q_{-} \equiv -eN_{-}\phi_{-}$, and the total charge, $Q = Q_{+} + Q_{-}$, of each macro-ion, Eq. (15). Similarly, Fig. 4(b) shows separately the cation charge density n_b^{+} , the anions charge density $-n_b^{-}$ (in units of e), and the bulk charge density of the salt, $n_b = n_b^{+} - n_b^{-}$. For small macro-ion concentrations, the positive and negative charge on each macro-ion barely change, and the changes in the cation and anion densities are small. However, as soon as $p_b N_{\pm} \approx n_0$, a clear transition ensues: the positive and negative charge of each macro-ion and the cation/anion density in the bulk sharply decrease, in agreement with the discussion above.

In Fig. 5 we plot the effective screening length of the 2S model, as a function of the bulk salt concentration, n_0 , at fixed p_b . We choose $P_0 \neq 0$ in order to have ions in solution with finite λ_{eff} in the absence of salt, $n_0 = 0$. When the chemical equilibrium constants are small ($p_b K_{\pm} \ll 1$, solid lines), λ_{eff} decreases monotonically and smoothly as function of n_0 , both in the symmetric and asymmetric cases. This decrease can be explained by the fact that for small K_{\pm} , the screening contribution from the charging of macro-ions is always small relatively to the increase of screening that comes from the mobile ions.

However, when the chemical equilibrium constants are very large ($p_b K_{\pm} > 1$, dashed lines), a different behavior is seen at the critical region, where $p_b N_{\pm} \approx n_0$. Above this point, *all* active sites are fully charged due to the large binding. In the asymmetric case, the screening length rapidly decreases as the macro-ions gain more and more charge. Once they are fully charged and saturation is reached, each added salt ion dissolve into the bulk. This is why we see a sudden change in the slop of λ_{eff} ,

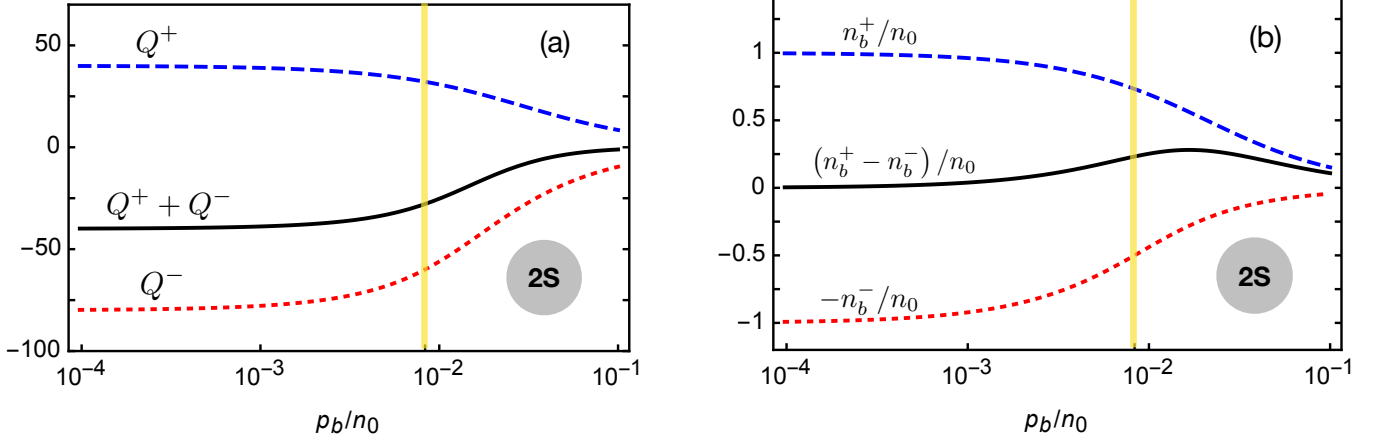


FIG. 4. (color online) Results for the 2S model. (a) The macro-ion effective charge as function of the macro-ion bulk concentration, p_b , rescaled by the bare salt concentration n_0 . Parameter values are: $N_{\pm} = 120$, $P_0 = 0$, $n_0 K_+ = 1/2$, and $n_0 K_- = 2$. The blue dashed line corresponds to positive charge, $Q_+ = N_+ \phi_+$, red dotted line to negative charge, $Q_- = -N_- \phi_- < 0$, and the black solid line to the overall charge $Q = Q_+ + Q_-$. All charges are in units of e , and the vertical yellow line denotes the transition in behavior at $n_0 = p_b N_{\pm}$. (b) The charge density of the salt ions as function of the concentration of the macro-ions, p_b , rescaled by n_0 , with the same parameters as in (a). All densities are rescaled by n_0 . The blue dashed line corresponds to positive charge density, n_b^+ , red dotted line to negative charge density, $-n_b^-$, and black solid line to overall charge density, $n_b^+ - n_b^-$.

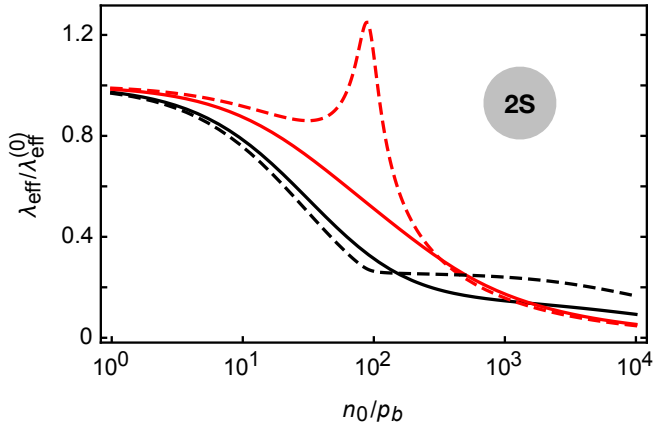


FIG. 5. (color online) $\lambda_{\text{eff}}/\lambda_{\text{eff}}^{(0)}$ for the 2S model, where $\lambda_{\text{eff}}^{(0)}$ is the screening length without added salt ($n_0 = 0$), as a function of the salt concentration n_0 , rescaled by the fixed macro-ion concentration, p_b . The red curves are symmetric cases: $p_b K_{\pm} = 1/100$ (full line), $p_b K_{\pm} = 2$ (dashed line), and the black curves correspond to the asymmetric cases: $p_b K_+ = 1/100$ and $K_- \rightarrow 0$ (full line), and $p_b K_+ = 2$ and $K_- \rightarrow 0$ (dashed line). Other system parameters are: $N_{\pm} = 120$ and $P_0 = 30$. Note that the values of $\lambda_{\text{eff}}^{(0)}$ are different for each curve.

similar to a phase transition in which a continuous change of a system parameter dramatically change the functional dependence of the screening.

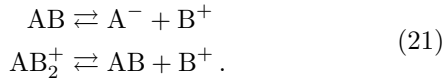
The symmetric case manifests an even more interesting behavior for the same limit of $K_{\pm} \gg 1$. At small salt concentrations, the macro-ions adsorb more and more cation/anion pairs. This results in an decrease

of λ_{eff} , followed by a sharp increase up to the point where $p_b N_{\pm} \simeq n_0$. This surprising phenomenon occurs because the contribution of symmetric macro-ions to the screening increases until they reach a maximal value when they are half filled. Then, the screening reduces until the point where the macro-ion sites are completely full (see Appendix A for more details). The increase is dramatic because after all macro-ions are half-filled the increase of salt concentration causes a *macroscopic* number of macro-ions to screen less for a small addition of salt. Once the macro-ion charge saturates, λ_{eff} drops, and the added salt ions stay dissolved in the solution rather than adsorb on the macro-ions.

C. The one-site (1S) model

Next, we consider a CR model that is referred to as the 1S model because the macro-ions have only one type of active sites. These sites are first taken as electroneutral, but they can either desorb or adsorb a cation, with a different free-energy cost. In our 1S model, there is only one type of active site that can undergo one of two competing processes: an association of an ion or a dissociation. Each of these processes has its own energy cost. In units of the elementary charge e , the overall charge of the site gets one of the three values: -1 , 0 or $+1$ (see Fig. 2(b)). This specific adsorption process involves just a single type of solution ion (positive) and one type of active site. It can be described by two chemical reaction

equations:



Such dissociation equilibrium can be used to model amphoteric (zwitterionic) charge processes [32, 48, 49]. It was studied experimentally in Ref. [50], on silica surfaces containing SiO^- groups that adsorb either one H^+ ion or two H^+ from the solution, and become SiOH or SiOH_2^+ , respectively.

We define the fraction of positively charged sites ϕ_+ and that of the negatively charged ones as ϕ_- . According to our model, ϕ_- is the fraction of sites that have released one cation to the solution, $1 - \phi_+ - \phi_-$ is the fraction of neutral sites, and ϕ_+ is the fraction of sites that adsorbed one cation from the solution. Therefore, the overall number of potentially dissociable positive ions on a macro-ion is $(1 - \phi_+ - \phi_-) + 2\phi_+ = 1 + \phi_+ - \phi_-$. The total number of active sites is N , and the free-energy gain of a neutral site adsorbing a cation is α_+ , while the free-energy gain of a negatively charged site adsorbing a cation is α_- .

The free energy of a single macro-ion is then given by,

$$\begin{aligned} g^{1\text{S}}(\psi, \phi_+, \phi_-) &= N(\phi_+ - \phi_-)e\psi \\ &\quad - N(\phi_+\alpha_+ - \phi_-\alpha_-) \\ &\quad - N(1 + \phi_+ - \phi_-)\mu_+ \\ &\quad + k_B T N \left[\phi_+ \ln \phi_+ + \phi_- \ln \phi_- \right. \\ &\quad \left. + (1 - \phi_+ - \phi_-) \ln (1 - \phi_+ - \phi_-) \right]. \end{aligned} \quad (22)$$

Two differences can be seen between the free energies, $g^{2\text{S}}$ and $g^{1\text{S}}$. The first one is the Lagrange multiplier $\mu_+ N (1 + \phi_+ - \phi_-)$ term in Eq. (22), which corresponds to the fact that cations are exchanged with the solution. The second difference is in the entropic part. It is modified because each site in the 1S model can be either positive, negative or neutral, and there is only one type of active sites.

The variation of F , Eq. (2), is now straightforward and is done using Eq. (22), along the same lines as for the 2S model above,

$$\phi_{\pm}(\psi) = \frac{Z_{\pm}^{1\text{S}}(\psi) - 1}{Z_{+}^{1\text{S}}(\psi) + Z_{-}^{1\text{S}}(\psi) - 1}. \quad (23)$$

where

$$\begin{aligned} Z_{+}^{1\text{S}} &= 1 + (n_b^+ K_+) e^{-\beta e \psi} \\ Z_{-}^{1\text{S}} &= 1 + (n_b^+ K_-)^{-1} e^{\beta e \psi}, \end{aligned} \quad (24)$$

and we made use of the appropriate chemical equilibrium constants, $K_{\pm} = a^3 \exp(\beta \alpha_{\pm})$, for the reactions as in Eq. (21). K_+ is the chemical equilibrium constant associated with a neutral AB site binding a cation and becoming AB_2^+ , while K_- is associated with A^- adsorbing

a cation and becoming a neutral AB. Finally, for simplicity, we omit throughout this subsection the superscript 1S.

Substituting the expression for ϕ_{\pm} [Eq. (23)] in Eq. (22), we get $g(\psi)$ in the form

$$g(\psi) = -N k_B T \ln [Z_+(\psi) + Z_-(\psi) - 1], \quad (25)$$

and substituting Eq. (25) into Eq. (5), gives the macro-ion concentration as

$$p(\psi) = p_b \frac{(Z_+(\psi) + Z_-(\psi) - 1)^N}{(Z_+(0) + Z_-(0) - 1)^N}. \quad (26)$$

The charge of each macro-ion for the 1S model is then

$$\begin{aligned} Q(\psi) &= eN(\phi_+ - \phi_-) \\ &= eN \left(\frac{Z_+(\psi) - Z_-(\psi)}{Z_+(\psi) + Z_-(\psi) - 1} \right), \end{aligned} \quad (27)$$

while the total charge density of macro-ions and salt monovalent ions is obtained by substituting Eqs. (26) and (27) into Eq. (6). This is similar to Eq. (17) of the 2S model, but for the 1S model, $p(\psi)$ and $Q(\psi)$ are given in Eqs. (26) and (27) above.

The relation between n_b^{\pm} and n_0 and p_b ensures an overall electro-neutrality as in

$$\begin{aligned} n_b^+ &= n_0 - p_b N (\phi_+ - \phi_-), \\ n_b^- &= n_0. \end{aligned} \quad (28)$$

The above equality, $n_b^- = n_0$, is valid because in the 1S model we explicitly assumed that the anions do not participate in the CR process of the macro-ions. Note also that in contrast to the 2S model, for the 1S model n_b^{\pm} do not depend on the number of initially charged sites (P_0). Recalling that the macro-ions are taken initially to be neutral, each macro-ion in the 1S model has N potentially dissociable groups that can be released into the solution, regardless of its initial occupancy.

D. Screening length for 1S model

We now discuss the screening phenomenology in the 1S model. Substituting Eqs. (16) and (28) into Eq. (19) results in the screening length of the form

$$\lambda_{\text{eff}} = \frac{\lambda_D}{\left(1 + \frac{1}{2} \frac{p_b N}{n_0} \left[(N-1) \left(\frac{Q(0)}{e} \right)^2 + 2\phi_-(0) \right] \right)^{1/2}}, \quad (29)$$

recalling that $Q(0)$ and $\phi(0)$ are bulk values taken at zero potential, $\psi = 0$. One immediate consequence is that λ_{eff} can only decrease relative to λ_D , to be distinguished from the 2S model, where both increase and decrease of the screening length are possible. More specifically, in the 1S model the macro-ion *cannot* adsorb pairs of positive and anions, which is the mechanism allowing an increase in the screening length in the 2S model.

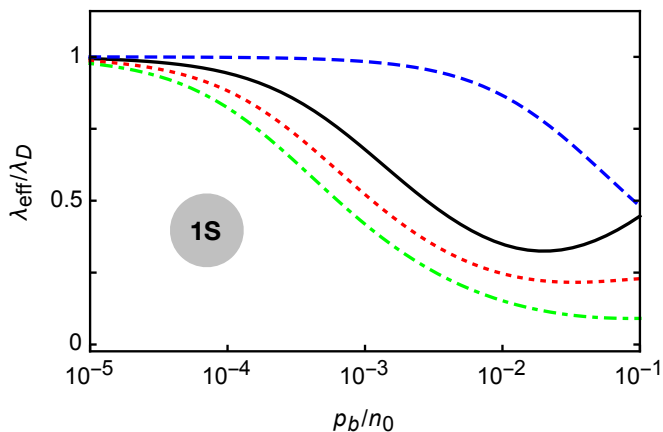


FIG. 6. (color online) Results for the 1S model. The screening length, λ_{eff} , rescaled by λ_D , the bare Debye screening length (no added macro-ions), plotted as function of the macro-ions bulk concentration, p_b , rescaled by the bare salt concentration n_0 . The four curves from top to bottom are: $n_0 K_- = 1$ (blue dashed line), $K_- \rightarrow \infty$ (black solid line), $n_0 K_- = 1/10$ (red dotted line), and $n_0 K_- = 1/100$ (green dot-dashed line). For all curves, $N = 100$ and $n_0 K_+ = 1$.

The term proportional to $Q(0)$ represents the charge asymmetry, and the larger it is, the larger the screening. However, to obtain full symmetry, *i.e.*, $Q(0) = 0$, the relation between the different constants is not as simple as in the 2S model. According to Eq. (27), the condition is that Z_+ and Z_- , defined in Eq. (24), should be equal to one another at $\psi = 0$. It then follows that there is no choice of K_+ and K_- which guarantees $Q(0) = 0$, regardless of the salt bulk concentration. Hence, the symmetry between positive and negative sites for a given bulk concentration does not guarantee that the symmetry will hold for a different concentration.

As for comparing donor and acceptor features, one should keep in mind that in the 1S model each macro-ion has initially (before it is added to the solution) N monovalent bound cations that can be released. Once placed in the solution, it can adsorb or release cations and remain with any number of them between 0 to $2N$. From the definition of ϕ_+ and ϕ_- in the 1S model, it follows that if $\phi_- > \phi_+$, then the macro-ion is a donor, while if $\phi_- < \phi_+$, it is an acceptor. The last term in Eq. (29), proportional to ϕ_- , is related to this feature: the larger ϕ_- is, the more likely it is that the macro-ion behaves as a donor and increases the screening.

In Fig. 6, λ_{eff} for the 1S model is plotted as a function of p_b (fixed n_0). The plotted blue, red and green curves behave similarly to the symmetric and asymmetric macro-ions in the 2S model, with large P_0 (see the green lines in Fig. 3). Similar behavior of these curves is attributed to the fact that the macro-ions donate a large amount of ions to the solution, whereas the black line describes a different case where neutral macro-ion sites cannot dissociate ($K_- \rightarrow \infty$). Therefore, they behave as acceptors, in accord with the observed non-monotonicity.

E. Disjoining pressure between two charged surfaces

We examine how the force (or equivalently the disjoining pressure) between two charged planar surfaces, bearing fixed surface charge density, is modified when they are embedded in a salt solution containing in addition charge-regulating macro-ions.

The disjoining pressure between two symmetric surfaces placed at $z = \pm d/2$, and each carrying a fixed charge density σ , is calculated by integrating the PB equation, Eq. (6), with the boundary conditions, $d\psi/dz|_{z=\pm d/2} = \pm 4\pi\sigma/\epsilon$. In fact the pressure between the surfaces is known to be [1, 44],

$$\Pi = -\frac{\epsilon}{8\pi}\psi'^2(z) + k_B T \sum_{i=\pm} [n_i(z) - n_b^i] + k_B T [p(z) - p_b]. \quad (30)$$

In equilibrium this pressure is a constant, independent of z , although each of its three terms are z -dependent. For convenience, we choose z to be at the midplane, $z = 0$, where by symmetry the electric field, $\psi'(0) = 0$, in Eq. (30), yielding a simplified form,

$$\Pi(z = 0) = k_B T \sum_{i=\pm} (n_i(0) - n_b^i) + k_B T (p(0) - p_b). \quad (31)$$

The disjoining pressure Π is then reduced to the difference in the ideal (van 't Hoff) osmotic pressure of three ionic species, calculated between the point at the midplane and the bulk.

In the Debye-Hückel (DH) limit, valid for $\lambda_{\text{eff}}^2/l_{GC}d \ll 1$, with the Gouy-Chapman length defined as $l_{GC} = \epsilon k_B T / 2\pi e |\sigma| = (1/2\pi l_B)(e/|\sigma|)$, the electrostatic potential ψ between two charged surfaces is obtained from the linearized PB equation, Eq. (18), and depends only on the effective screening length, λ_{eff} [1]. The electrostatic potential determines the salt ions and macro-ion concentrations, which in turn determine Π . Consequently, we expect the disjoining pressure to exhibit, a non-monotonic dependence on system parameters, stemming from the λ_{eff} behavior. Intuitively, we can argue that the screening decreases the range of the interaction between the two surfaces, and in turn this decreases the disjoining pressure.

In Fig. 7, we plot the disjoining pressure, $\Pi(d)$, between the two charged surfaces, as function of d , the inter-plate distance. The pressure dependence is obtained by solving numerically the full PB equation for the 2S and 1S models, and, for comparison we also plot $\Pi(d)$ for the DH approximation. As is clear from the figure, the disjoining pressure always decreases monotonically with d , just as is expected for simple ionic solutions [1]. We note that for large d , where the electrostatic potential is small, the full PB and the DH curves coincide. For the 2S model, the addition of macro-ions can either increase or decrease Π for all values of d , as can be seen by comparing the plots with macro-ions (red and green) with

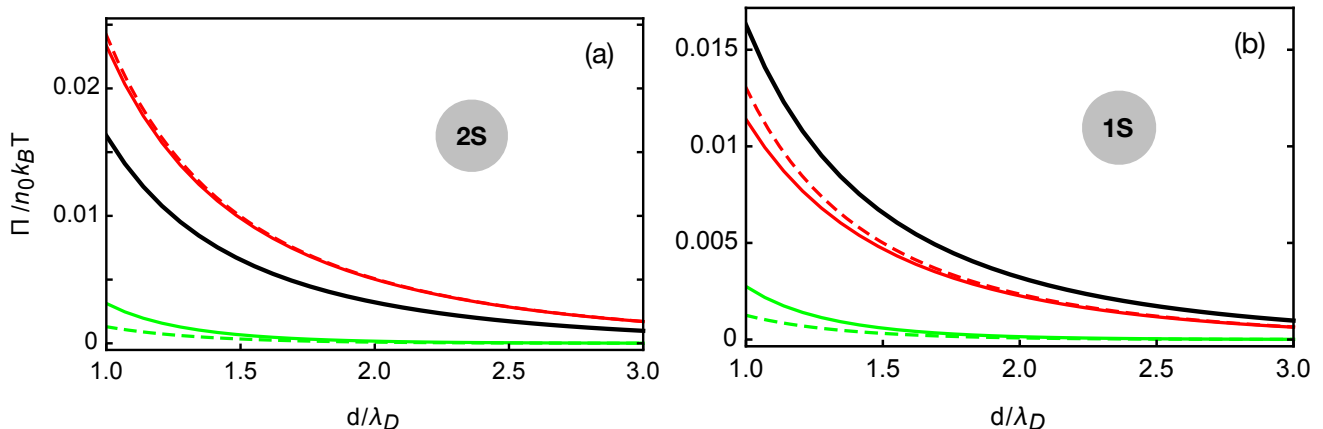


FIG. 7. (color online) Disjoining pressure Π (rescaled by $n_0 k_B T$), as function of the distance between the surfaces, d (rescaled by λ_D). Solid lines correspond to exact PB theory, while dashed lines to the DH approximation, where the electrostatic potential is given by $\psi(z) = -(2\lambda_{\text{eff}}/l_{\text{GC}}) \cosh(z/\lambda_{\text{eff}}) / \sinh(d/2\lambda_{\text{eff}})$ (a) Results for the 2S model, where the green lines correspond to asymmetric case, $K_+ \rightarrow 0$ and $n_0 K_- = 10$, and the red lines to symmetric case, $n_0 K_{\pm} = 10$. The black line corresponds to no added macro-ions, $p_b = 0$, and is plotted for comparison. The other parameter values are: $l_{\text{GC}}/\lambda_D = 30$, $p_b/n_0 = 0.01$, $N_{\pm} = 40$ and $P_0 = 0$. (b) The same plot as in (a), but for the 1S model. Parameter values are: $N = 80$, $K_+ \rightarrow \infty$ and $n_0 K_- = 1$ (green lines), and $n_0 K_{\pm} = 1$ (red lines). The black line corresponds to $p_b = 0$ (no macro-ions), and is plotted for comparison. The parameters l_{GC}/λ_D and p_b/n_0 have the same values as in (a).

the curve without them (black). This agrees with the result obtained in Sec. III B, since the screening length can increase or decrease, as function of the concentration of the macro-ions, p_b . On the other hand, in the 1S model, the screening always increases (see Sec. III D), so the resulting Π always decreases as function of p_b , for all values of d .

We conclude this section by showing in Fig. 8 the disjoining pressure in the 2S model for a fixed value of d as function of p_b/n_0 , for different charge asymmetry cases (as defined in Sec. III B). We focus on the case where $P_0 = 0$, for which the non-monotonicity effect is the largest. At low macro-ion concentration, symmetric macro-ions increase the inter-plate pressure, in agreement with the results presented in Fig. 6, while the asymmetric macro-ions decrease it. When $N_{\pm} p_b \approx n_0$, a sharp transition in the behavior is seen and the original trend changes its sign, in agreement with the behavior of the screening length that is depicted in Fig. 3 (black lines). In the symmetric case, another transition is seen for higher macro-ion concentration, where the pressure begins to increase again. This transition cannot be simply understood by the screening length behavior, but involves non-linear effects due to the charged boundaries. Therefore, the charge regulation mechanism contains further rich phenomena beyond what is explored in this paper, especially those related to higher-order effects.

IV. CONCLUSIONS

In this work we have addressed the role of mobile and complex charge-regulating (CR) macro-ions with differ-

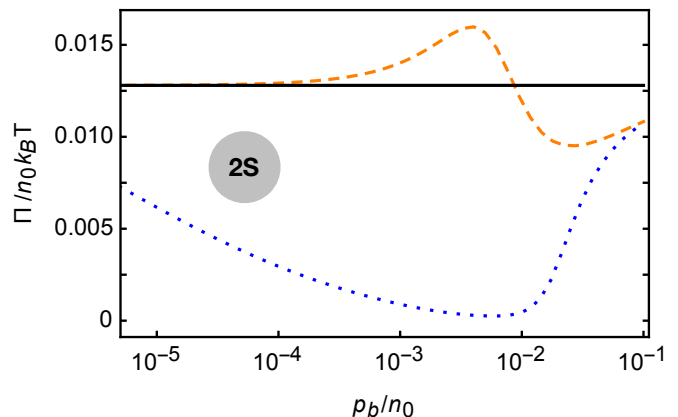


FIG. 8. (color online) Disjoining pressure Π in the 2S model (rescaled by $n_0 k_B T$), as function of the macro-ion concentration p_b (rescaled by the bare salt n_0). Parameter values are: $N_+ = 120$, $N_- = 60$ (blue dotted line), and $N_+ = 120$, $N_- = 0$ (red dashed line). The reference pressure of no macro-ions is shown as the black line. Other parameter values are: $d/\lambda_D = 2$, $d/l_{\text{GC}} = 2/15$, $n_0 K_{\pm} = 5$ and $P_0 = 0$.

ent types of CR mechanisms, dissolved in a simple salt solution. Our goal is to highlight the collective effects, and to treat on par the translational degrees of freedom of the charge regulating macro-ions with those of the simple salt ions [41]. This more general treatment leads to quite unexpected outcomes, and points out to rich patterns exhibited by complex colloid solutions. In particular, we scrutinized the resulting screening properties as well as the interactions between two charged interfaces immersed in CR colloid solution.

Two CR models are studied in detail: the two-site (2S) and one-site (1S) models. The 2S model has two uncorrelated sites. One of them can adsorb a cation and the other can adsorb an anion. The situation is somewhat different in the 1S model, where there is only one type of sites that can either adsorb or desorb a cation. As can be seen in this work, the two models give quite different results.

Our most important finding is the anomalous non-monotonic dependence of the effective screening length (λ_{eff}) on the bulk concentrations of the macro-ions p_b , and the salt n_0 . As can be seen in Figs. 3-6, the screening displays even more unexpected features, in addition to those already identified for a variant of the 2S model in Ref. [41]. In addition, we investigate the properties of the disjoining pressure, Π , between two planar surfaces with fixed charges. As is clear from Fig. 7, the non-monotonic screening is reflected in the behavior of the disjoining pressure as function of macro-ion concentration, p_b , at a fixed value of the inter-surface separation, d .

A detailed analysis shows that for the 2S and 1S models the dependence of λ_{eff} on the salt and/or macro-ion concentrations is governed by two important characteristics of the macro-ion CR process: (i) the balance between the different association processes, which can be quantified by whether the macro-ion prefers to have a neutral overall charge (symmetric state), or a non-zero value (asymmetric state), and (ii) the donor/acceptor propensity that relates to the macro-ion preference to either release ions to the bathing solution, or acquire ions from it (and sometimes it also depends on initial solution preparation conditions).

In both 1S and 2S models, macro-ions that prefer an overall non-zero charge ($Q \neq 0$), *i.e.*, exhibiting an *asymmetric* charging process, display increased screening. Consequently, they reduce the disjoining pressure between the charged bounding surfaces when compared with the case of no added macro-ions at the same solution conditions. Contrary, symmetric macro-ions prefer an overall close to zero charge ($Q \approx 0$). In the 2S model this is achieved by adsorption of cation-anion pairs, which decreases the effective screening. In the 1S model, it is achieved by releasing and adsorbing the same amount of positive ions, still increasing the screening, but to a lesser extent than for the asymmetric case.

Apart from the overall charge (a)symmetry, the CR models introduced in our study exhibit a behavior that is related to their donor/acceptor propensity for exchanging salt ions with the bathing solution. Acceptor macro-ions tend to absorb more cations and anions from the bathing solution than they release, while donor macro-ions donate more ions to the bathing solution. The preference to be either an acceptor or a donor depends on the details of the CR mechanism. Comparing the donor/acceptor propensity behavior, we are able to find that acceptor macro-ions present a more interesting case. Increasing their concentration leads to a transition from a state where most of the ions are in the bulk, to a state where most of them

are adsorb by the macro-ions. This transition leads to non-monotonic dependence of the screening length, λ_{eff} , on the salt and the macro-ions bulk concentrations.

An unexpected phenomenon is observed in the screening properties of symmetric macro-ions in the 2S model. At first glance, one may assume that such macro-ions do not contribute to the screening, as they carry an overall zero charge at zero electrostatic potential. However, we demonstrate that this is not the case, and further show that the macro-ions have small contribution to the screening for zero or full occupation, while they have a large contribution for half occupancy (see Eq. (A5)). This property has a novel non-intuitive implication. In extreme cases, it causes the screening length to exhibits a rapid increase with the addition of salt. This behavior, besides being contrary to the behavior expected for the regular λ_D , is somewhat reminiscent to a phase transitions in the sense that a small change in a system parameter (n_0) inflicts a macroscopic response of λ_{eff} (see Fig. 5).

Quite recently, some experiments have been conducted on charge regulation of non-polar colloids [42], and are pertinent to our analysis [41]. In the experimental system, the colloid macro-ions are dispersed in hydrophobic dodecane (non-polar) solvent and carry a charge that can self-adjust due to dissociation/association of weakly-ionized surface groups. The effective charge of the colloid macro-ions is estimated from fits to scattering experimental results of concentrated colloidal dispersions, and one of the main findings is a non-monotonic behavior as a function of the colloidal concentration. While in a broad sense, this experimental system is close to our theoretical ramifications, the details of the charging mechanism and the relation between the experimentally determined effective charge and our own effective colloidal charge, Q , are at present not entirely sorted out, and are left for follow-up studies.

In this work, we advocate a line of reasoning that charge regulation is essential in modeling complex macro-ion dispersed in ionic solutions. More detailed quantitative comparison between theory and experiment requires further understanding of the charging mechanism in experiments. These as well as specific protein segregation and adsorption phenomena, will be investigated in future studies.

Acknowledgements. This work was supported in part by the ISF-NSFC (Israel-China) joint research program under Grant No. 885/15. RP would like to thank the School of Physics and Astronomy at Tel Aviv University for its hospitality, and is grateful for the Sackler Scholar award and the Spirit and Michael Shoal fellowship, within the framework of the Mortimer and Raymond Sackler Institute of Advanced Studies at Tel Aviv University. TM acknowledges the support from the Blavatnik postdoctoral fellowship programme, and RP was supported by

the 1000-Talents Program of the Chinese Foreign Experts Bureau.

Appendix A: Electrostatic screening by symmetric macro-ions (2S model)

We concentrate on symmetric (neutral on average) macro-ions and show how in the 2S model their screening depends on the number of cation and anion pairs that the macro-ions adsorb. We assume complete symmetry: $K_{\pm} = K$, $N_{\pm} = N$, $n_b^{\pm} = n_b$, and fix the bulk salt concentration n_0 , such that the only variable is $\phi_{\pm}(0) \equiv \phi(0)$, the fraction of occupied sites at zero electrostatic potential (which is the same for positive and negative sites).

From the symmetry of the macro-ions, $Q(0) = 0$. Substituting this condition in Eqs. (19) and (16), it follows that the contribution of the macro-ions to the screening length is

$$\lambda_{\text{MI}}^{-2} = -\frac{4\pi p_b}{\epsilon} \left. \frac{Q(\psi)}{\partial\psi} \right|_{\psi=0}. \quad (\text{A1})$$

In order to find $Q(\psi)$ in terms of $\phi(0)$, we first invert the relation

$$\phi(0) = \frac{n_b K}{1 + n_b K}, \quad (\text{A2})$$

and obtain

$$n_b K = \frac{\phi(0)}{1 - \phi(0)}. \quad (\text{A3})$$

Substituting Eq. (A3) in Eq. (15), we get

$$\begin{aligned} Q(\psi) &= Q_+(\psi) + Q_-(\psi) \\ &= \frac{Ne\phi(0)e^{-\beta e\psi}}{1 - \phi(0)(1 - e^{-\beta e\psi})} - \frac{Ne\phi(0)e^{\beta e\psi}}{1 - \phi(0)(1 - e^{\beta e\psi})} \end{aligned} \quad (\text{A4})$$

and Eq. (A1) becomes

$$\lambda_{\text{MI}}^{-2} = \frac{8\pi p_b}{\epsilon} N\phi(0)(1 - \phi(0)). \quad (\text{A5})$$

Equation (A5) shows that when the overall charge is zero, the screening length of the macro-ions is proportional to the variance of the binomial distribution, $N\phi(0)(1 - \phi(0))$. The variance of this positive/negative charge distribution is maximal when $\phi(0) = 1/2$ and minimal when $\phi(0) = 0$ (or 1). Indeed, macro-ions that are “half full” are free to adsorb or release charges, whereas completely “full” or completely “empty” macro-ions have less freedom; they can only release ions or only adsorb them, which reduces their ability to screen electrostatic interactions.

Furthermore, if we take k symmetric ions, each with occupancy fraction of $\phi(0)$, their screening is larger (smaller λ_{MI}) than for a single macro-ion with an occupancy fraction of $k\phi(0)$, because the relation $k\phi(0)(1 - \phi(0)) > k\phi(0)(1 - k\phi(0))$ holds for any $k > 1$. We finally remark that the above calculation is done for a fixed bulk density of ions, and the effect of the macro-ions on the bathing solution was not considered.

-
- [1] T. Markovich, D. Andelman and R. Podgornik, Chapter 9 in: *Handbook of Lipid Membranes*, ed. by C. Safinya and J. Raedler, Taylor & Francis, to be published, (2018).
- [2] L. Woods, D. Dalvit, A. Tkatchenko, P. Rodriguez-Lopez, A. Rodriguez, and R. Podgornik, *Rev. Mod. Phys.*, 2016, **88**, 045003.
- [3] J. N. Israelachvili, *Intermolecular and Surface Forces*, 3rd ed, Academic Press, Burlington, 2011.
- [4] M. Perutz, *Science*, 1978, **201**, 1187-1191.
- [5] A. Warshel, P. Sharma, M. Kato, and W. Parson, *Biochim. Biophys. Acta*, 2006, **1764**, 1647-1676.
- [6] I. Gitlin, J. D. Carbeck, and G. M. *Angew. Chem. Int. Ed.*, 2006, **45**, 3022-3060.
- [7] E. J. W. Verwey and J. T. G. Overbeek, *Theory of the stability of lyophobic colloids*. Elsevier, Amsterdam, 1948.
- [8] S. H. Behrens and M. Borkovec, *J. Phys. Chem. B*, 1999 **103**, 2918-2928.
- [9] S. H. Behrens and M. Borkovec, *J. Chem. Phys.*, 1999, **111**, 382-385.
- [10] M. Lund and B. Jönsson, *Biochemistry*, 2005, **44**, 5722-5727.
- [11] F. L. Barroso da Silva and B. Jönsson *Soft Matter*, 2009, **5**, 2862-2868.
- [12] Y. Nozaki and C. Tanford, *Methods Enzymol.*, 1967, **11**, 715-734.
- [13] A. L. Bozic and R. Podgornik, *Biophys. J.*, 2017, **113**, 1454-1465.
- [14] K. U. Linderstrøm-Lang, *Medd. Carlsberg Lab.*, 1924, **15**, 1-28.
- [15] B. W. Ninham and V. A. Parsegian, *J. Theor. Biol.*, 1971, **31**, 405-428.
- [16] D. Chan, J. W. Perram, L. R. White and T. W. Healy, *J. Chem. Soc. Faraday Trans. I*, 1975, **71**, 1046-1057.
- [17] D. C. Prieve E. Ruckenstein, *J. Theor. Biol.*, 1976, **56**, 205-228.
- [18] R. Pericet-Camara, G. Papastavrou, S.H. Behrens and M. Borkovec, *J. Phys. Chem. B*, 2004, **108**, 19467-19475.
- [19] H. H. von Grunberg, *J. Colloid Interface Sci.*, 1999, **219**, 339-344.
- [20] R. Podgornik and V. A. Parsegian, *J. Chem. Phys.*, 1995, **99**, 9491-9496.
- [21] M. L. Henle, C. D. Santangelo, D. M. Patel and P. A. Pincus, *Europhys. Lett.*, 2004, **66**, 284-290.
- [22] G. S. Longo, M. Olvera de la Cruz and I. Szleifer, *Soft Matter*, 2012, **8**, 1344-1354.
- [23] G. S. Longo, M. Olvera de la Cruz and I. Szleifer, *ACS Nano*, 2013, **7**, 2693-2704.
- [24] N. Adzic and R. Podgornik, *Euro. Phys. J. E*, 2014, **37**,

- 49.
- [25] A. C. Maggs and R. Podgornik, *EPL*, 2014, **108** 68003.
- [26] T. Markovich, D. Andelman and R. Podgornik, *EPL*, 2014, **106**, 16002.
- [27] H. Diamant and D. Andelman, *J. Phys. Chem.*, 1996, **100**, 13732.
- [28] P. M. Biesheuvel, *J. Coll. Interface Sci.*, 2004, **257**, 514-522.
- [29] D. Ben-Yaakov, D. Andelman, R. Podgornik, D. Harries, *Curr. Opin. Colloid & Interface Sci.*, 2011, **16**, 542-550.
- [30] T. Markovich, D. Andelman, and R. Podgornik, *EPL*, 2016, **113**, 26004.
- [31] R. J. Nap, A. L. Bozic, I. Szleifer, and R. Podgornik, *Biophys. J.*, 2014, **107** 1970-1979.
- [32] D. Chan, T. W. Healy and L. R. White, *J. Chem. Soc. Faraday Trans. I*, 1976, **72**, 2844.
- [33] B. W. Ninham and V. A. Parsegian, *J. Theoretical Biology*, 1971, **31**, 405.
- [34] J. C. Everts, S. Samin and R. van Roij, *Phys. Rev. Lett.*, 2016, **117**, 098002.
- [35] C. Pasquier, M. Vazdar, J. Forsman, P. Jungwirth, and M. Lund, *J. Phys. Chem. B*, 2017, **121**, 3000.
- [36] M. Lund and B. Jönsson, *Biochemistry*, 2005, **44** 5722.
- [37] M. Borkovec, J. Daicic and G. J. Koper, *Proc. Natl. Acad. Sci.*, 1997, **94**, 3499.
- [38] M. Ullner, B. Jönsson, and P. Widmark, *J. Chem. Phys.*, 1994, **100**, 3365.
- [39] M. Borkovec, B. Jönsson, and G. J. Koper, *Ionization processes and proton binding in polyprotic systems: small molecules, proteins, interfaces, and polyelectrolytes. Surface and colloid science*. Springer US, 2001.
- [40] N. Boon and R. van Roij, *J. Coll. Interf. Sci.*, 2012, **385**, 66.
- [41] T. Markovich, D. Andelman, and R. Podgornik, *EPL*, 2017, **120**, 26001.
- [42] J. E. Hallett, D. A. J. Gillespie, R. M. Richardson, and P. Bartlett, *Soft matter*, 2018, **14**, 331-343.
- [43] H.P. Erickson, *Biol. Proced. Online.*, 2009, **11** 32-51.
- [44] A. C. Maggs and R. Podgornik, *Soft matter*, 2016, **12**, 1219.
- [45] D. Harries, R. Podgornik, V. A. Parsegian, E. May-Or and D. Andelman, *J. Chem. Phys.*, 2006, **124**, 224702.
- [46] T. H. Healy and L. R. White, *Adv. Coll. Interf. Sci.*, 1978, **9**, 303.
- [47] I. Borukhov, D. Andelman, and H. Orland, *Euro. Phys. J. B*, 1998, **5**, 869.
- [48] R. Ettelaie and R. Buscall, *Adv. Coll. Interf. Sci.*, 1995, **61**, 131.
- [49] P. M. Biesheuvel, *J. Coll. Interf. Sci.*, 2004, **275**, 514.
- [50] J. Morag, M. Dishon and U. Sivan, *Langmuir*, 2013, **29**, 6317.